NASA TECHNICAL NOTE

NASA TN D-4942

NASA TN D-4942



# MATCHED-CONIC SOLUTIONS TO ROUND-TRIP INTERPLANETARY TRAJECTORY PROBLEMS THAT INSURE STATE-VECTOR CONTINUITY AT ALL BOUNDARIES

*by Victor R. Bond*

*Manned Spacecraft Center*
*Houston, Texas*

NATIONAL AERONAUTICS AND SPACE ADMINISTRATION • WASHINGTON, D. C. • JANUARY 1969

# MATCHED-CONIC SOLUTIONS TO ROUND-TRIP INTERPLANETARY TRAJECTORY PROBLEMS THAT INSURE STATE-VECTOR CONTINUITY AT ALL BOUNDARIES

By Victor R. Bond

Manned Spacecraft Center
Houston, Texas

NATIONAL AERONAUTICS AND SPACE ADMINISTRATION

For sale by the Clearinghouse for Federal Scientific and Technical Information
Springfield, Virginia 22151 – CFSTI price $3.00

## ABSTRACT

A technique is presented for computing the matched-conic solutions of interplanetary trajectories for use as reference trajectories in guidance and navigation simulations. Continuity in position, velocity, and time at the sphere of influence is insured. The chief advantage of the matching technique is its capability of being adapted to several mission types. Examples are presented of the types of missions considered: the free-flyby mission, the powered-flyby mission, and the stopover mission with a parking orbit about the target planet.

CONTENTS

## TABLES



## FIGURES

# MATCHED-CONIC SOLUTIONS TO ROUND-TRIP INTERPLANETARY TRAJECTORY PROBLEMS THAT INSURE STATE-VECTOR CONTINUITY AT ALL BOUNDARIES

By Victor R. Bond
Manned Spacecraft Center

## SUMMARY

A technique is presented for computing the matched-conic solutions of interplanetary trajectories for use as reference trajectories in guidance and navigation simulations. The matching is made, with continuity in position, velocity, and time at the sphere-of-influence boundaries insured. The technique, which satisfies inflight constraints at the target planet, is extended to several types of round-trip planetary missions. The types of missions considered are the free-flyby mission, the powered-flyby mission, and the stopover mission with a parking orbit about the target planet. An example is presented of each type of mission.

## INTRODUCTION

Matched-conic, or analytic, solutions to interplanetary trajectory problems have been used successfully in mission studies and as first approximations to more precise solutions. In reference 1, the need was stated for continuous conic solutions to interplanetary trajectory problems. The primary use of such continuous solutions is in the area of guidance and navigation error analyses. A technique was also presented in reference 1 for generating interplanetary trajectories that are continuous at the sphere of influence; however, the development was confined to one-way or single-leg trajectories. In manned interplanetary applications, the return trajectory must also be computed; in general, the departure and return portions of the trajectory cannot be computed independently. The two trajectories are related by conditions at the target planet that cannot be specified arbitrarily.

Other matched-conic techniques for solving the round-trip interplanetary trajectory problem have been used. The circumlunar matched-conic trajectory technique presented in reference 2 and repeated later in reference 3, is probably one of the earliest techniques used. Several types of round-trip trajectories are discussed in reference 4. Reference 5 is a discussion of round-trip missions and a presentation of a method for determining if an additional velocity increment on either the departure or the return trajectory, or on both trajectories, will reduce the total velocity requirements for the mission.

In this report, some of the mathematical techniques that are required for matched-conic trajectories to meet specified boundary conditions at the departure, target, and return planets are presented. Boundary conditions at the planets are discussed in references 1 and 3. A detailed discussion of a process for matching the heliocentric and planetocentric trajectories at the sphere-of-influence boundaries will also appear in this report. A different matching technique was presented in reference 1. None of references 1 to 5, with the exception of references 2 and 3 which are concerned with circumlunar trajectories, present a detailed description of the matching of the departure and return legs within the target-planet sphere of influence, although the assumption might be made that the matching is implicitly considered, if not explained. The matching of the departure and return legs will generally involve variation of either or both flight times until certain constraints at the target planet have been satisfied and the matching has been completed.

The precision with which the matching at and within the spheres of influence is made is determined by the usage that the results of the solution will have. For studies in which only minimum velocity requirements are desired, little or no matching is required for the single-leg trajectory. To find the round-trip trajectory with minimum velocity requirements, the trip times that satisfy mission constraints at the target planet must be provided first. The constraints arise from the type of mission (e.g., free flyby, powered flyby, stopover with parking orbit, etc.). (The term "free flyby" refers to a trajectory in which no velocity change is applied in the vicinity of a planet while flying by the planet; "powered flyby" refers to a trajectory in which a velocity change is applied in the vicinity of a planet while flying by the planet.)

There are applications, however, for which a more precise matching is required. For guidance and navigation error analyses, it is desirable to have a reference or nominal trajectory that is continuous in both position and velocity. The matching technique described in this report is presented for use in guidance and navigation error analyses that require continuity in position and velocity. The equations of motion in guidance and navigation analyses are linearized by series expansions about the reference trajectory. The first-order terms of the series expansions yield the sensitivity coefficients for propagating errors along the reference trajectory. The sensitivity coefficients are discussed and derived in reference 3 and will not be considered in this report.

In the section of this paper entitled "Example Problems," an example problem will be presented for each of the three types of trajectory solutions. The first two examples were chosen from recently published literature. The author wishes to acknowledge E. W. Henry of the Manned Spacecraft Center for suggesting the third example problem.

## SYMBOLS

$a$ semimajor axis

$a_{ij}$ matrix elements

$e$ eccentricity

| | |
|---|---|
| $f$ | true anomaly |
| $f_\infty$ | true anomaly of hyperbolic asymptote |
| $H$ | argument of hyperbolic sine or cosine (analogous to eccentric anomaly) |
| $h$ | altitude above planet surface |
| $\hat{h}$ | unit vector along angular momentum |
| $i$ | inclination with respect to planet equator (which may be arbitrarily defined) |
| $\hat{i}, \hat{j}, \hat{k}$ | orthogonal set of unit vectors |
| $J_2$ | coefficient of second zonal harmonic of planetary potential function |
| $k$ | index specifying maximum or minimum periapsis declination |
| $m$ | integer |
| $\hat{n}$ | unit vector along ascending node of orbit and planet equator |
| $P$ | computed period |
| $p$ | semilatus rectum |
| $R_B$ | equatorial radius of a planet |
| $\bar{R}$ | position vector relative to Sun |
| $r$ | position relative to planet |
| $\bar{r}$ | position vector relative to planet |
| $\hat{S}$ | unit vector along hyperbolic asymptote |
| $T$ | Julian or calendar date |
| $t$ | time from zero |
| $t_s$ | stay time at the target planet |
| $\bar{V}$ | velocity vector relative to Sun |
| $v$ | velocity relative to planet |

$v_\infty$ hyperbolic excess velocity

$\vec{v}$ velocity vector relative to planet

$\vec{v}_\infty$ hyperbolic excess velocity vector

X, Y, Z Cartesian coordinates of the position vector

y constraint function

$\alpha$ right ascension of $\hat{S}$

$\Delta t$ specified time increment

$\delta$ declination of $\hat{S}$

$\delta t$ computed time increment

$\eta$ $\cos^{-1}\left(\frac{1}{e}\right)$

$$\kappa = \cos^{-1}\left(\frac{-\vec{v}_{\infty, A, T}}{v_{\infty, A, T}} \cdot \frac{\vec{v}_{\infty, D, T}}{v_{\infty, D, T}}\right)$$

$\mu$ gravitational constant

$\nu$ one-half the angle between the arrival and the departure hyperbolic excess velocities at the target planet

$\sigma$ $\sin^{-1}\left(\frac{\tan \delta}{\tan i}\right)$

$\tau$ designates either $t_R$ or $t_T$ in equations (54) to (59)

$\phi$ angle between the vectors $\hat{n}$ and $\hat{S}$

$\Omega$ right ascension of the ascending node

$\omega$ argument of periapsis

Subscripts:

A arrival planet

D departure planet

k index to resolve nodal ambiguity

P planet

R return planet (usually the same as the departure planet, but not required to be the same)

T target planet

$\pi$ periapsis (or minimum distance from planet)

Superscripts:

* sphere-of-influence boundary

' evaluated from heliocentric conic

+ evaluated from planetocentric conic

c computed quantity

(j) quantity evaluated during jth iteration, where $j = 0, 1, \ldots$

Operator:

$(\dot{})$ derivative with respect to time

## COMPUTATIONAL TECHNIQUE

The techniques discussed in this report have been programed in FORTRAN V for the Univac 1108 digital computer. Several types of trajectory problems are considered. The first problem considered will be to obtain the single-leg matched-conic trajectory between any two arbitrary planets. A flow chart describing the matching process for this trajectory solution is shown in figure 1. The single-leg matched-conic solution is required in order to obtain the round-trip trajectory solutions that will be discussed in the following order: (1) the free-flyby trajectory; (2) the parking-orbit (stopover) trajectory about an oblate planet; and (3) the coincident periapsis trajectory, which will yield either the powered-flyby trajectory or the parking orbit about a spherical homogeneous planet.

The computer program that has been developed has a limited search capability. That is, data such as departure date and approximate flight time are normally input to the program, and the input flight times are then changed by iteration until the constraints, boundary conditions, and matching criteria are satisfied. The iterations usually occur in two modes, as shown in figure 2. The first mode, the gross iteration mode, utilizes heliocentric conics to satisfy constraints at the target planet. During the gross iteration mode, no matching of position and velocity vectors at the spheres of influence is achieved. After the constraints have been satisfied in the gross iteration mode, the tolerances are reduced, and the fine iteration mode begins. In the fine

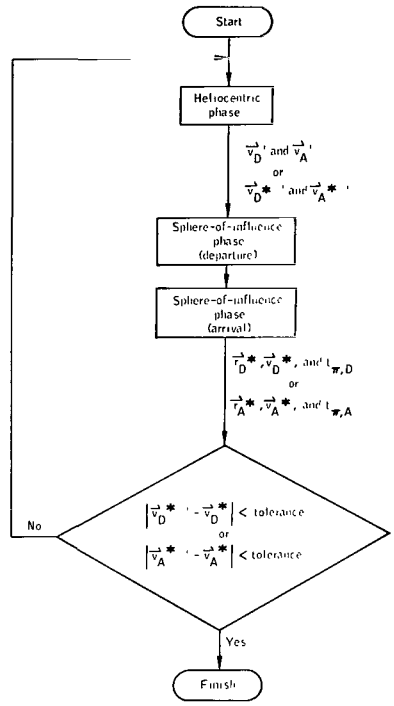


Figure 1. - Computation for a single-leg (one way) interplanetary matched-conic trajectory.

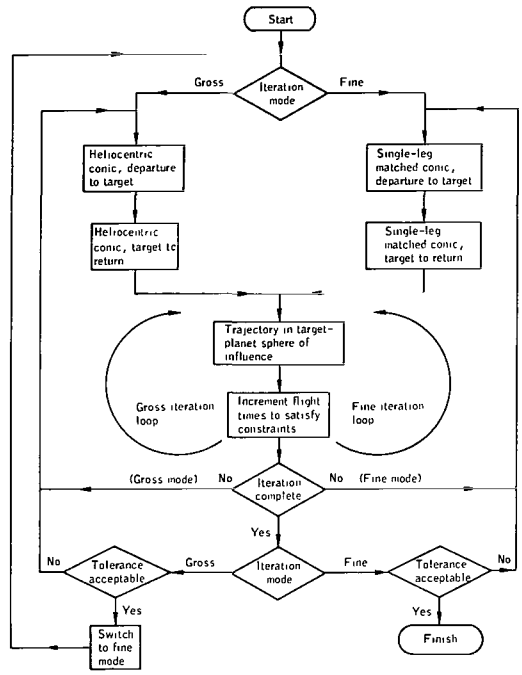


Figure 2. - Computation for round-trip interplanetary matched-conic trajectories.

interation mode, single-leg matched conics are used to satisfy the same set of constraints as were satisfied in the gross iteration mode. The end result of the fine iteration is that the constraints and all the other boundary conditions are satisfied.

## DETERMINATION OF THE MATCHED-CONIC TRAJECTORY BETWEEN TWO ARBITRARILY CHOSEN PLANETS

To obtain the matched-conic trajectory between two arbitrarily chosen planets (referred to as the single-leg matched-conic solution), $T_D$ is designated as the periapsis departure date, $T_A$ is designated as the periapsis arrival date, $i_D$ is designated as the inclination of the trajectory with respect to a planetocentric coordinate system at the departure planet, $i_A$ is designated as the inclination of the trajectory with respect to a planetocentric coordinate system at the arrival planet, $h_{\pi,D}$ is designated as the periapsis altitude at the departure planet, and $h_{\pi,A}$ is designated as the periapsis altitude at the arrival planet. To resolve the ambiguity of the trajectory in each planetocentric sphere of influence, $k_D$ is designated as an index that specifies the maximum ($k = 1$) or minimum ($k = 0$) periapsis declination at the departure planet, and $k_A$ is designated as an index that specifies the maximum ($k = 1$) or minimum ($k = 0$) periapsis declination at the arrival planet. For a given set of the specified quantities

$T_D$, $T_A$, $i_D$, $i_A$, $h_{\pi,D}$ and $h_{\pi,A}$, there are four possible solutions corresponding to the four possible combinations of $k_D$ and $k_A$. The bounds on the specified inclinations $i_D$ and $i_A$ and the indices $k_D$ and $k_A$ will be discussed in the section of this report entitled "The Planetocentric Phase."

## The Heliocentric Phase

If the date of arrival or departure from a planet is given, then the heliocentric position and velocity of the planet may be computed from the planet ephemeris. At the departure planet, the position and velocity vectors are $\vec{R}_{P,D}(T_D)$ and $\vec{V}_{P,D}(T_D)$; and at the arrival planet, the position and velocity vectors are $\vec{R}_{P,A}(T_A)$ and $\vec{V}_{P,A}(T_A)$. If the spacecraft is at a known position $\vec{r}_D(T_D)$ or $\vec{r}_A(T_A)$ from the departure or arrival planets at the same date, then the heliocentric positions of the spacecraft are

$$\vec{R}_D(T_D) = \vec{r}_D(T_D) + \vec{R}_{P,D}(T_D) \tag{1}$$

and

$$\vec{R}_A(T_A) = \vec{r}_A(T_A) + \vec{R}_{P,A}(T_A) \tag{2}$$

The position vectors $\vec{R}_D$ and $\vec{R}_A$ and the time $T_A - T_D$ are used to determine the heliocentric velocities $\vec{V}_D$ and $\vec{V}_A$ in the vicinity of the departure and arrival planets. This calculation is known as Lambert's problem and is documented in reference 3. The velocities of the spacecraft with respect to the planet are then

$$\vec{v}_D'(T_D) = \vec{V}_D(T_D) - \vec{V}_{P,D}(T_D) \tag{3}$$

and

$$\vec{v}_A'(T_A) = \vec{V}_A(T_A) - \vec{V}_{P,A}(T_A) \tag{4}$$

When the procedure is used for the first time in the solution of a single-leg trajectory, $\vec{r}_D$ and $\vec{r}_A$ are zero, and the spacecraft is assumed to be at the center of the planets at the dates $T_D$ and $T_A$. After the planetocentric computations, good estimates for $\vec{r}_D{}^*$ and $\vec{r}_A{}^*$ are obtained. The superscript * indicates that $\vec{r}_D$ and $\vec{r}_A$ are taken at the planet sphere of influence.

The dates at the spheres of influence must also be corrected at arrival and departure. Therefore, the vectors

$$\vec{R}_D{}^*\left(T_D{}^*\right) = \vec{r}_D{}^*\left(T_D{}^*\right) + \vec{R}_{P,D}\left(T_D{}^*\right) \tag{5}$$

and

$$\vec{R}_A{}^*\left(T_A{}^*\right) = \vec{r}_A{}^*\left(T_A{}^*\right) + \vec{R}_{P,A}\left(T_A{}^*\right) \tag{6}$$

where $T_D{}^* = T_D + t_{\pi,D}$ and $T_A{}^* = T_A + t_{\pi,A}$ are now used in the solution of Lambert's problem to obtain $\vec{V}_D{}^*$ and $\vec{V}_A{}^*$. The velocities at the spheres of influence are

$$\vec{v}_D{}^{*\,\prime}\left(T_D{}^*\right) = \vec{V}_D{}^*\left(T_D{}^*\right) - \vec{V}_{P,D}\left(T_D{}^*\right) \tag{7}$$

and

$$\vec{v}_A{}^{*\,\prime}\left(T_A{}^*\right) = \vec{V}_A{}^*\left(T_A{}^*\right) - \vec{V}_{P,A}\left(T_A{}^*\right) \tag{8}$$

The superscript ' indicates velocities computed from heliocentric orbits, with the planets assumed to be massless.

## The Planetocentric Phase

To compute the trajectory within a planetocentric sphere of influence, the following vectors are specified:

1. The position vector $\vec{r}^*$ of the spacecraft with respect to the planet at the sphere of influence was computed during the last sphere-of-influence computation and remained unchanged during the heliocentric phase.

2. The velocity vector $\vec{v}^{*\prime}$ of the spacecraft with respect to the planet at the sphere of influence was computed from equations (7) and (8) during the heliocentric phase.

3. The inclination of the hyperbola with respect to the planet equator (or to some other arbitrary plane) is designated as i.

4. The periapsis altitude of the hyperbola is designated as $h_\pi$.

5. An index that specifies which node is to be chosen is designated by k.

The computations for departure and arrival are similar, and the subscripts D and A are omitted, except where they are necessary for clarity. During the first computation of the trajectory in a planetocentric phase, only the magnitude of the position $\vec{r}^*$ is known, and the velocity $\vec{v}^{*\prime}$ must be approximated by the velocity of the spacecraft relative to the planet and must be evaluated at the center of the planet assumed massless, using equations (3) and (4). This evaluation causes no special problem, since $\vec{v}_D'$ and $\vec{v}_A'$ are good approximations to the sphere-of-influence velocities $\vec{v}_D^{*\prime}$ and $\vec{v}_D^{*\prime}$. The purpose for requiring both $\vec{r}^*$ and $\vec{v}^{*\prime}$ is to allow the $\vec{v}_\infty$ vector to be computed. During the first computation in a sphere of influence, $\vec{v}_\infty$ must be approximated, although during subsequent passes, $\vec{v}_\infty$ is computed exactly.

When the spacecraft is assumed to be at the center of the planet $\left(\vec{r}_D = 0 \text{ or } \vec{r}_A = 0\right)$, an approximate computation of the hyperbolic asymptote is made from

$$\hat{S} = \pm \frac{\vec{v}'}{v'} \tag{9}$$

where the plus sign is used for departure and the minus sign is used for arrival.

The magnitude of the hyperbolic excess velocity is

$$v_\infty = \sqrt{(v')^2 - \frac{2\mu}{r^*}} \tag{10}$$

When the spacecraft is at the sphere of influence, the hyperbolic excess velocity and asymptote are computed exactly (ref. 3) from

$$\vec{v}_\infty = \left\{ \frac{\vec{r}^* \cdot \vec{v}^{*\prime}}{p^* r^*} \left[ 1 - \cos\left(f_\infty - f^*\right) \right] - \frac{1}{r^*} \sqrt{\frac{\mu}{p^*}} \sin\left(f_\infty - f^*\right) \right\} \vec{r}^* + \left\{ 1 - \frac{r^*}{p^*} \left[ 1 - \cos\left(f_\infty - f^*\right) \right] \right\} \vec{v}^{*\prime} \tag{11}$$

where

$$\left.\begin{aligned} \cos f_\infty &= \frac{-1}{e^*} \qquad p^* = \frac{\left| \vec{r}^* \times \vec{v}^{*\prime} \right|^2}{\mu} \qquad e^* = \sqrt{1 - \frac{p^*}{a^*}} \\ a^* &= \left[ \frac{2}{r^*} - \frac{\left(v^{*\prime}\right)^2}{\mu} \right]^{-1} \qquad \cos f^* = \frac{1}{e^*} \left( \frac{p^*}{r^*} - 1 \right) \end{aligned}\right\} \tag{12}$$

$f_\infty - f^* > 0$ for departure, and $f_\infty - f^* < 0$ for arrival.

The hyperbolic excess velocity is

$$v_\infty = \left| \vec{v}_\infty \right| \tag{13}$$

and the hyperbolic asymptote is

$$\hat{S} = \pm \frac{\vec{v}_\infty}{v_\infty} \tag{14}$$

The trajectory within the sphere of influence is given initially by $\vec{r}^*$ and $\vec{v}^*$, and has orbital parameters that are not related to the specified orbital parameters. When the trajectory is propagated to infinity, using equation (11), the inclination and periapsis radius that would be found from $\vec{r}^*$ and $\vec{v}^*$ lose all meaning. Therefore, the specified periapsis conditions are now imposed.

The only problem remaining in the sphere-of-influence phase is to determine the position and velocity vectors $\vec{r}_\pi$ and $\vec{v}_\pi$ at periapsis and the time $t_\pi$ from periapsis to the sphere of influence, using the quantities $v_\infty$, $\hat{S}$, $i$, $h_\pi$, and $r^*$. The vectors $\vec{r}_\pi$ and $\vec{v}_\pi$ and the time $t_\pi$ are easily derived from figures 3 and 4, and the results for departure are stated as

$$\vec{r}_{\pi,D} = r_{\pi,D}\left[\cos\eta\hat{S}_D - \sin\eta\left(\hat{h}\times\hat{S}_D\right)\right] \tag{15}$$

and

$$\vec{v}_{\pi,D} = v_{\pi,D}\left[\sin\eta\hat{S}_D + \cos\eta\left(\hat{h}\times\hat{S}_D\right)\right] \tag{16}$$

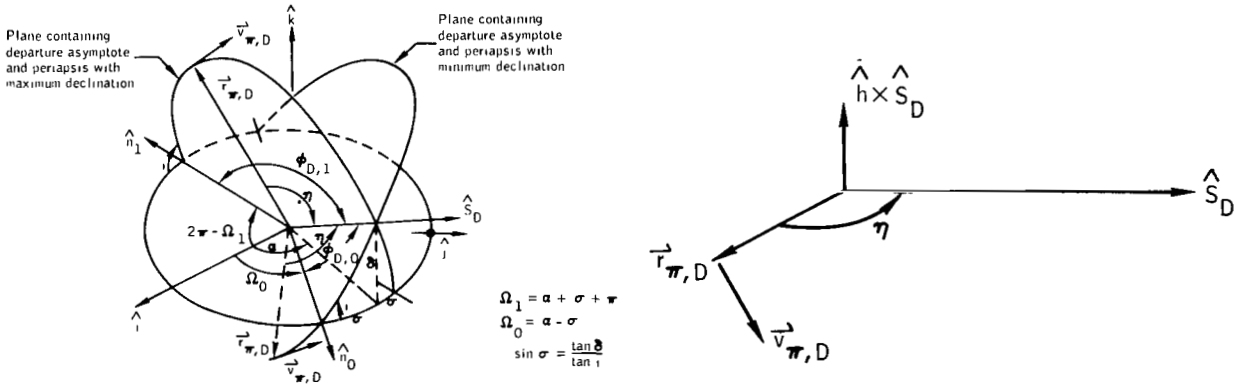


(a) Spherical geometry.

(b) Planar geometry ($\hat{h}$ extending out of the page).

Figure 3. - Relation between the periapsis vectors and the hyperbolic asymptotes at the departure planet.

For arrival, the results are stated as

$$\vec{r}_{\pi,A} = r_{\pi,A}\left[\cos\eta\hat{S}_A + \sin\eta\left(\hat{h}\times\hat{S}_A\right)\right] \tag{17}$$

and

$$\vec{v}_{\pi,A} = v_{\pi,A}\left[-\sin\eta\hat{S}_A + \cos\eta\left(\hat{h}\times\hat{S}_A\right)\right] \tag{18}$$

where

$$\left.\begin{aligned} r_\pi &= h_\pi + \text{planet radius} & v_\pi &= \sqrt{\mu\left(\frac{2}{r_\pi} - \frac{1}{a}\right)} \\ a &= \frac{-\mu}{v_\infty^2} & e &= 1 - \frac{r_\pi}{a} \\ \cos\eta &= -\frac{1}{e} & \frac{\pi}{2} &< \eta < \pi \\ \hat{h} &= \hat{i}\sin\Omega\sin i - \hat{j}\cos\Omega\sin i + \hat{k}\cos i \end{aligned}\right\} \tag{19}$$

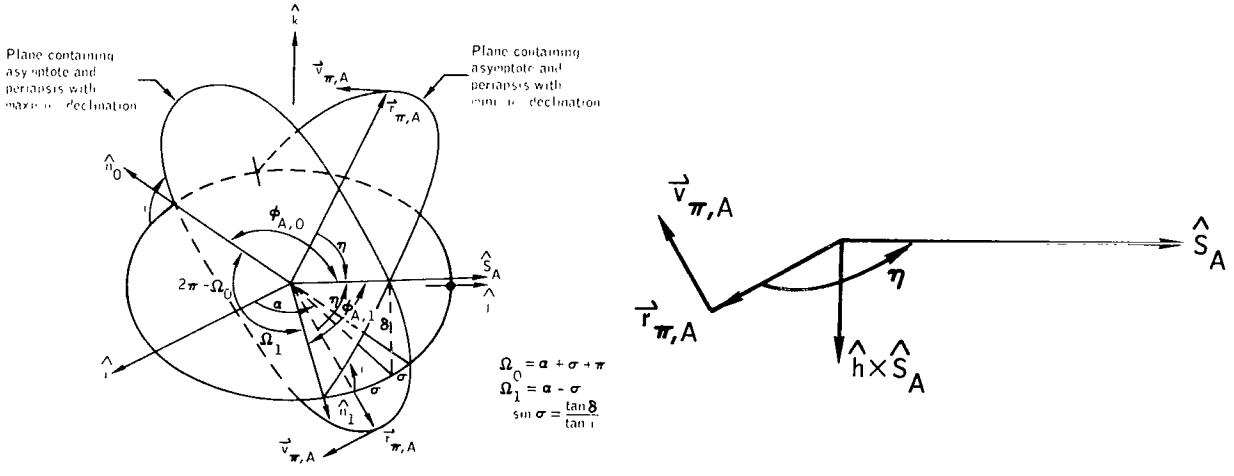


(a) Spherical geometry.

(b) Planar geometry ($\hat{h}$ extending into the page).

Figure 4. - Relation between the periapsis vectors and the hyperbolic asymptotes at the arrival planet.

The right ascension $\Omega$ of the ascending node is ambiguous. From figures 3 and 4

$$\Omega_k = \begin{cases} \alpha - \sigma \\ \alpha + \sigma + \pi \end{cases} \tag{20}$$

where $\alpha$ is the right ascension of the asymptote. For departure, the nodes that give the maximum (k = 1) and minimum (k = 0) periapsis declinations are

$$\left.\begin{aligned} \Omega_1 &= \alpha + \sigma + \pi \\ \Omega_0 &= \alpha - \sigma \end{aligned}\right\} \tag{21}$$

and for arrival, the nodes that give the maximum and minimum periapsis declinations are

$$\left.\begin{aligned} \Omega_1 &= \alpha - \sigma \\ \Omega_0 &= \alpha + \sigma + \pi \end{aligned}\right\} \tag{22}$$

where

$$\sigma = \sin^{-1}\left(\frac{\tan \delta}{\tan i}\right) \tag{23}$$

and $\delta$ is the declination of the asymptote. Equation (23) indicates that the permissible inclinations are bounded by $\pi - |\delta| > i > |\delta|$.

The time from periapsis to the sphere of influence is

$$t_\pi = \pm\sqrt{\frac{-a^3}{\mu}}\,(e \sinh H - H) \tag{24}$$

where the plus sign is used for departure, and the minus sign is used for arrival. Also

$$H = \cosh^{-1}\left[\frac{1}{e}\left(1 - \frac{r^*}{a}\right)\right] \tag{25}$$

The sphere-of-influence position and velocity vectors that satisfy the specified inclination and periapsis altitude are now computed (ref. 3) from

$$\vec{r}^{\,*+} = r^*\left(\frac{\vec{r}_\pi}{r_\pi}\cos f + \frac{\vec{v}_\pi}{v_\pi}\sin f\right) \tag{26}$$

and

$$\vec{v}^{\,*} = \sqrt{\frac{\mu}{p}}\left[-\frac{\vec{r}_\pi}{r_\pi}\sin f + \frac{\vec{v}_\pi}{v_\pi}(e + \cos f)\right] \tag{27}$$

where

$$\left.\begin{aligned} &\cos f = \left(\frac{p}{r^*} - 1\right)\frac{1}{e} \qquad p = a\left(1 - e^2\right) \\ &\frac{\pi}{2} < f < \pi \text{ for departure} \\ &\pi < f < \frac{3\pi}{2} \text{ for arrival} \end{aligned}\right\} \tag{28}$$

In equation (26), $\vec{r}^{\,*}$ has an additional superscript + to indicate that the position vector in equation (26) differs from the original $\vec{r}^{\,*}$ of equation (11). The vector $\vec{r}^{\,*+}$ is used in equations (5) and (6) to determine the heliocentric position vectors of the spacecraft at the spheres of influence.

## The Matching Process to Obtain a Single-Leg Trajectory

The process of matching the position and velocity vectors at the spheres of influence to obtain the single-leg matched conic is accomplished by using a successive approximation technique. The logic of the computation technique is also presented in figure 1 and in the following:

1. If the departure and arrival dates $T_D$ and $T_A$ are given, the relative velocity vectors $\bar{v}_D'$ and $\bar{v}_A'$ are provided by the heliocentric solution, with the spacecraft assumed to be at the center of the departure and arrival planets at the dates $T_D$ and $T_A$, respectively.

2. If the relative velocity vectors $\bar{v}_D'$ and $\bar{v}_A'$ are given or if the sphere-of-influence velocities $\bar{v}_D^{*\prime}$ and $\bar{v}_A^{*\prime}$ are computed in the heliocentric phase, along with the inclinations $i_D$ and $i_A$ and the altitudes $h_{\pi,D}$ and $h_{\pi,A}$, the position and velocity vectors $\bar{r}_D^{*+}$, $\bar{v}_D^{*}$, $\bar{r}_A^{*+}$, and $\bar{v}_A^{*}$ at the spheres of influence are computed in the planetocentric phases. The times $t_{\pi,D}$ and $t_{\pi,A}$ from each periapsis to each sphere of influence are also computed.

3. The heliocentric phase is now repeated, adjusting the heliocentric positions of the spacecraft and the departure and arrival times according to equations (5) and (6). The velocities $\bar{v}_D^{*\prime}$ and $\bar{v}_A^{*\prime}$ at the arrival and departure spheres of influence, respectively, are obtained from the adjusted solution.

4. The velocity errors $\left|\bar{v}_D^{*\prime} - \bar{v}_D^{*}\right|$ and $\left|\bar{v}_A^{*\prime} - \bar{v}_A^{*}\right|$ are now computed. If the errors are less than the tolerance, the solution is assumed to be converged. If the tolerance is not met, then steps 2 and 3 are repeated.

The matching process may be visualized by considering that the date $T^*$ and the position vector $\bar{r}^*$ at the sphere of influence are changed until $\bar{v}^* = \bar{v}^{*\prime}$. This procedure for matching is similar to the procedure used in reference 1.

## THE FREE-FLYBY MATCHED-CONIC MODE

To compute the orbital parameters for the free-flyby mode, $T_D$ is designated as the periapsis departure date, $i_D$ is designated as the inclination at the departure planet, $i_R$ is designated as the inclination at the return planet, $h_{\pi,D}$ is designated as periapsis altitude at the departure planet, $h_{\pi,R}$ is designated as periapsis altitude

at the return planet, $h_{\pi, T}$ is designated as the periapsis altitude at the target planet, $k_D$ is designated as the maximum (k = 1) or minimum (k = 0) periapsis declination at the departure planet, and $k_R$ is designated as the maximum or minimum periapsis declination at the return planet. The flight times $t_T$ (time from departure to target) and $t_R$ (time from target to return) are dependent variables and require initial guesses. An additional constraint must be satisfied in order to attain the free-flyby trajectory: the velocity magnitudes of the arrival and departure hyperbolic excess velocities must be equal. The flight times must be computed by a numerical iteration procedure so that the flyby constraint is satisfied and the computed periapsis altitude is equal to the specified value.

In the first iteration, only heliocentric conics are used, and all the boundary conditions except $T_D$ and $h_{\pi, T}$ are ignored. This mode is called the gross iteration mode and is done to improve the flight times, to determine the flyby inclination $i_T$, and to resolve the nodal ambiguity.

When the flyby constraints are approximately satisfied, the computation proceeds to the fine iteration mode. In this mode, all boundary conditions, flyby constraints, and continuity at the spheres of influence are satisfied. The trajectories used in this mode are single-leg matched-conic trajectories, the solutions of which are described in a previous section. The computation for both the gross and the fine iteration modes is illustrated schematically in figure 2.

## Computation of the Free-Flyby Trajectory Within the Target-Planet Sphere of Influence

It is assumed that the hyperbolic excess velocities $\bar{v}_{\infty, A, T}$ and $\bar{v}_{\infty, D, T}$ have been computed and that the magnitudes of these velocities are approximately equal. The hyperbolic excess velocities may be computed by either of the methods described in the section of this report entitled "The Planetocentric Phase," depending upon whether the velocities are relative velocities and the planets are assumed to be massless or upon whether the position and velocity vectors at the sphere of influence are known.

As shown in figure 5, the plane of the orbit is computed from

$$\hat{h}_T = \frac{\bar{v}_{\infty, A, T} \times \bar{v}_{\infty, D, T}}{\left| \bar{v}_{\infty, A, T} \times \bar{v}_{\infty, D, T} \right|} \tag{29}$$

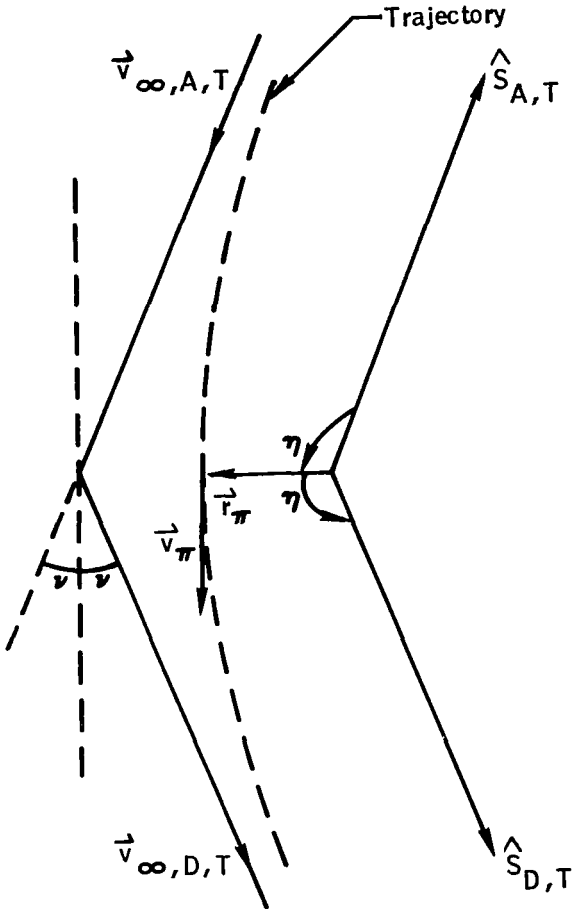


Figure 5. - Geometry of the free-flyby hyperbolic trajectory.

The inclination is found from

$$\cos i_T = \hat{k} \cdot \hat{h}_T \tag{30}$$

The angle $2\nu$ between $\vec{v}_{\infty, A, T}$ and $\vec{v}_{\infty, D, T}$ is found from

$$\sin 2\nu = \frac{\left|\vec{v}_{\infty, A, T} \times \vec{v}_{\infty, D, T}\right|}{\left(v_{\infty, A, T}\right)\left(v_{\infty, D, T}\right)} \tag{31}$$

The radius of periapsis is computed from

$$r_{\pi, T}{}^{c} = a(1 - \csc \nu) \tag{32}$$

where

$$a = -\frac{\mu}{\left(v_{\infty, D, T}\right)^2} = -\frac{\mu}{\left(v_{\infty, A, T}\right)^2} \tag{33}$$

It should be emphasized that $r_{\pi, T}{}^{c}$ is a computed value because in the free-flyby mode, $r_{\pi, T}$ is actually specified. In the description of the iteration technique given in the following section of this report, details will be given concerning how the flight times $t_T$ and $t_R$ are adjusted so that the difference $r_{\pi, T} - r_{\pi, T}{}^{c}$ vanishes.

The inclination $i_T$ is to be used in the single-leg computations in place of a specified $i_T$. An additional quantity k is required in order to determine which ambiguous node is to be chosen. The decision about which k to use is resolved by examining figures 3 and 4.

The nodal vector $\hat{n}_k$ is

$$\hat{n}_k = \frac{\hat{k} \times \hat{h}_T}{\sin i_T} \tag{34}$$

For the departure leg

$$\cos \phi_D = \hat{n}_k \cdot \hat{S}_{D,T} \tag{35}$$

and $\cos \phi_D$ must always be negative for a maximum (k = 1) periapsis declination and positive for a minimum (k = 0) periapsis declination. If $\cos \phi_D < 0$, $\Omega_1 = \alpha + \sigma + \pi$; if $\cos \phi_D > 0$, $\Omega_0 = \alpha - \sigma$. Similarly, for the arrival leg

$$\cos \phi_A = \hat{n}_k \cdot \hat{S}_{A,T} \tag{36}$$

The $\cos \phi_A$ must always be positive for a maximum (k = 1) periapsis declination and negative for a minimum (k = 0) periapsis declination. If $\cos \phi_A > 0$, $\Omega_1 = \alpha - \sigma$; if $\cos \phi_A < 0$, $\Omega_0 = \alpha + \sigma + \pi$.

## Iteration Technique for Computing the Flight Times for the Free-Flyby Trajectory

In the solution for the free-flyby trajectory the flight times $t_T$ and $t_R$ must satisfy the constraints

$$y_1 = v_{\infty,A,T} - v_{\infty,D,T} = 0 \tag{37}$$

$$y_2 = h_{\pi,T} - h_{\pi,T}^{c} = 0 \tag{38}$$

The periapsis altitude $h_{\pi, T}^{c}$ is computed from equation (32), and $h_{\pi, T}$ is specified. During the gross iteration mode, when only the constraints in equations (37) and (38) are to be satisfied, velocities that reduce the final errors in equations (37) and (38) to 0.1 km/hr and 0.1 kilometer, respectively, are provided from equations (3) and (4). When this accuracy has been obtained, the fine iteration begins, and the flyby constraints and all other boundary values must now be satisfied. In the fine iteration mode, the more precise velocities computed from equation (10) are used. The fine iteration mode is continued until the errors in equations (37) and (38) are 0.01 km/hr and 0.01 kilometer, respectively.

The variables $y_1$ and $y_2$ may be considered functions of the flight times $t_T$ and $t_R$.

$$y_1 = y_1\left(t_T, t_R\right) \tag{39}$$

$$y_2 = y_2\left(t_T, t_R\right) \tag{40}$$

The solution to these equations may be done numerically by the Newton-Raphson method, as described in reference 6. Symbolically, the solution may be written as

$$t_T = t_T^{(0)} + \delta t_T \tag{41}$$

and

$$t_R = t_R^{(0)} + \delta t_R \tag{42}$$

where

$$\begin{pmatrix} \delta t_T \\ \delta t_R \end{pmatrix} = \frac{-1}{a_{11}a_{22} - a_{12}a_{21}} \begin{bmatrix} a_{22} & -a_{12} \\ -a_{21} & a_{11} \end{bmatrix} \begin{pmatrix} y_1^{(0)} \\ y_2^{(0)} \end{pmatrix} \tag{43}$$

The matrix elements $a_{ij}$ are defined by the partial derivatives

$$\left.\begin{aligned} a_{11} &= \frac{\partial y_1}{\partial t_T} & a_{12} &= \frac{\partial y_1}{\partial t_R} \\ a_{21} &= \frac{\partial y_2}{\partial t_T} & a_{22} &= \frac{\partial y_2}{\partial t_R} \end{aligned}\right\} \tag{44}$$

The derivatives are difficult to obtain in closed form, but they may be obtained numerically by the following procedure:

1. A pair of trajectories (that is, one trajectory from the departure planet to the target planet and another trajectory from the target planet to the return planet) is computed, using the first-guess times $t_T^{(0)}$ and $t_R^{(0)}$. Then, the residuals

$$y_1^{(0)} = y_1\left[t_T^{(0)}, t_R^{(0)}\right] \tag{45}$$

and

$$y_2^{(0)} = y_2\left[t_T^{(0)}, t_R^{(0)}\right] \tag{46}$$

are formed.

2. A second pair of trajectories is computed, using the times $t_T^{(1)} = t_T^{(0)} + \Delta t_T$ and $t_R^{(0)}$; that is, $t_T^{(0)}$ is incremented by $\Delta t_T$, and $t_R^{(0)}$ is held constant. Then, the residuals

$$y_1^{(1)} = y_1\left[t_T^{(1)}, t_R^{(0)}\right] \tag{47}$$

and

$$y_2^{(1)} = y_2\left[\overline{t_T}^{(1)}, t_R^{(0)}\right] \tag{48}$$

are formed.

3. A third pair of trajectories is computed, using the times $t_T^{(0)}$ $t_R^{(2)} = t_R^{(0)} + \Delta t_R$, and the residuals

$$y_1^{(2)} = y_1\left[\overline{t_T}^{(0)}, t_R^{(2)}\right] \tag{49}$$

and

$$y_2^{(2)} = y_2\left[\overline{t_T}^{(0)}, t_R^{(2)}\right] \tag{50}$$

are formed. The partial derivatives may now be approximated.

$$\left.\begin{aligned} a_{11} &= \frac{y_1^{(1)} - y_1^{(0)}}{\Delta t_T} & a_{12} &= \frac{y_1^{(2)} - y_1^{(0)}}{\Delta t_R} \\ a_{21} &= \frac{y_2^{(1)} - y_2^{(0)}}{\Delta t_T} & a_{22} &= \frac{y_2^{(2)} - y_2^{(0)}}{\Delta t_R} \end{aligned}\right\} \tag{51}$$

4. A fourth pair of trajectories is computed, using the corrected times from equations (41) and (42). If equations (37) and (38) are still not satisfied to some tolerance, then the entire procedure is repeated.

## MATCHED-CONIC TRAJECTORY WITH A PARKING ORBIT ABOUT AN OBLATE PLANET

To obtain a matched-conic trajectory with a parking orbit about an oblate planet, $T_D$ is designated as the periapsis departure date, $T_R$ is designated as the periapsis return date, $T_T$ is designated as the periapsis target date, $i_D$ is designated as the inclination at the departure planet, $i_R$ is designated as the inclination at the return planet, $h_{\pi, D}$ is designated as the periapsis altitude at the departure planet, $h_{\pi, R}$ is designated as the periapsis altitude at the return planet, $h_{\pi, T}$ is designated as the periapsis altitude at the target planet, $t_s$ is designated as the stay time at the target planet, $k_D$ is designated as the maximum (k = 1) or minimum (k = 0) periapsis declination at the departure planet, and $k_R$ is designated as the maximum or minimum periapsis declination at the return planet. In addition, the constraint that the stay time be equal to an integral number of orbital periods must be imposed.

It is assumed that the hyperbolic excess velocities $\vec{v}_{\infty, A, T}$ and $\vec{v}_{\infty, D, T}$ have been computed. These velocity vectors were computed, with a specified stay time $t_s$ at the target planet assumed. If the radius of periapsis at the target $r_{\pi, T}$ is also specified, then it is possible to find several parking-orbit solutions that contain $\vec{v}_{\infty, A, T}$ initially and that contain $v_{\infty, D, T}$ at the end of the stay time (fig. 6). The rotation of the parking orbit is accomplished by the secular perturbations that arise from the oblateness of the target planet. From reference 7, the rates of change of the node and of the argument of periapsis of the parking orbit are

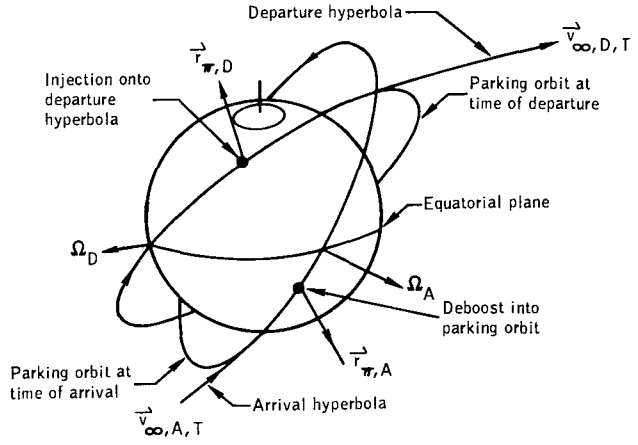


Figure 6. - Geometry of the parking orbit at the time of arrival and departure.

$$\dot{\Omega} = -\frac{3\sqrt{\frac{\mu}{a^3}}J_2R_B^2}{2a^2\left(1-e^2\right)^2}\cos i \qquad (52)$$

and

$$\dot{\omega} = -\frac{3\sqrt{\frac{\mu}{a^3}}J_2R_B^2}{2a^2\left(1-e^2\right)^2}\left(\frac{5}{2}\sin^2 i - 2\right) \qquad (53)$$

where $J_2$ is the second zonal harmonic of the planetary potential function and $R_B$ is the equatorial radius of the planet.

Not only are the solutions nonunique; they must be found numerically. The technique used to obtain the solutions is discussed at length in reference 8 and will not be repeated here. It is sufficient to say that the technique yields several pairs of inclinations and eccentricities for the parking orbit.

The solutions obtained in reference 8 did not impose the constraint that the stay time be equal to an integral number of orbital periods. When this condition is imposed, a unique solution is obtained. The condition may be expressed as

$$t_s - mP^c = 0 \tag{54}$$

where $m$ is the integer part of $t_s/P^c$. The computed period $P^c$ is the anomalistic period, that is, the time required to go from periapsis to periapsis. Since the mean motion also undergoes a secular perturbation, the anomalistic period is not the same as the period in the corresponding two-body problem. From reference 7, the perturbed mean motion $2\pi/P^c$ and thus the computed period are found from

$$\frac{2\pi}{P^c} = \sqrt{\frac{\mu}{a^3}}\left[1 - \frac{3J_2R_B^2}{2a^2\left(1 - e^2\right)^{3/2}}\left(\frac{3}{2}\sin^2 i - 1\right)\right] \tag{55}$$

The constraint in equation (54) can be satisfied either by permitting $t_T$ to be free and constraining the total flight time, or by permitting $t_R$ to be free and constraining $t_T$.

If $\tau$ is used to designate either $t_R$ or $t_T$, the constraint given by equation (54) may then be written as

$$y(\tau) = t_s - mP^c = 0 \tag{56}$$

The time $\tau$ may be found iteratively by the Newton-Raphson technique

$$\tau^{(1)} = \tau^{(0)} - \frac{y^{(0)}(\tau)}{\frac{dy}{d\tau}} \tag{57}$$

where

$$\frac{dy}{d\tau} = \frac{y^{(1)} - y^{(0)}}{\Delta\tau} \tag{58}$$

The Newton-Raphson technique requires two pairs of trajectories in order to establish the derivative in equation (58). The first iteration is a gross iteration; that is, no attempt is made to solve all boundary conditions or to force continuity at the spheres of influence. Succeeding iterations are fine iterations requiring all boundary conditions to be matched and requiring continuity at the sphere of influence. The only boundary condition that is not specified is the inclination at the target planet, which is found from equations (52) and (53).

## MATCHED-CONIC TRAJECTORY WITH COINCIDENT PERIAPSIS POSITIONS AT THE TARGET PLANET

To obtain the matched-conic trajectory with coincident periapsis positions at the target planet, the same specifications are required as were required in the previous section. If the stay time is not equal to zero, then the solution yields the parking orbit about a spherical homogeneous planet, with the further restriction that the stay time, if not zero, must not be less than the stay time of a circular orbit at the specified altitude $h_{\pi, T}$. If the stay time is specified to be zero, then the solution yields a powered-flyby trajectory with an impulse applied at the periapsis. Both modes may be handled conveniently by the same information, since both modes have the common constraint that the periapsis position vectors for arrival and departure at the target be coincident. As in the previous section, either $t_T$ or $t_R$ may be left free so that the periapsis altitude $h_{\pi, T}$ may be specified.

It is assumed that the hyperbolic excess velocity vectors $\bar{v}_{\infty, A, T}$ and $\bar{v}_{\infty, D, T}$ have been computed. The inclination and the choice of the node to be used are determined exactly as in the computation of the free-flyby trajectory. The radius of periapsis must be computed differently, since the matched-conic trajectory with coincident periapsis positions at the target planet is discontinuous in velocity at periapsis.

The solution for the radius of periapsis starts with the requirement that the periapsides of the arrival and departure hyperbolas must be coincident. In figure 7, it is shown that this requirement may be expressed as

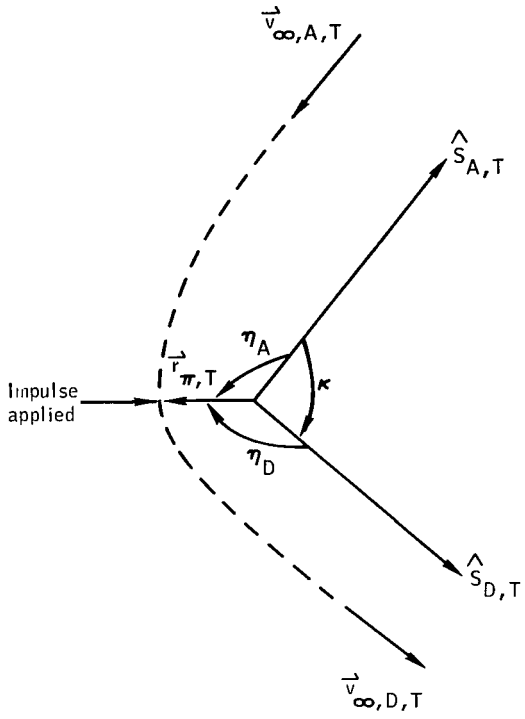


Figure 7. - Coincident periapsides condition.

$$\eta_A + \eta_D + \kappa = 2\pi \tag{59}$$

where

$$\kappa = \cos^{-1}\left(\frac{-\vec{v}_{\infty,A,T}}{v_{\infty,A,T}} \cdot \frac{\vec{v}_{\infty,D,T}}{v_{\infty,D,T}}\right) \tag{60}$$

$$\eta_A = \cos^{-1}\left(\frac{-1}{1 + \frac{\left(r_{\pi,T}{}^{c}\right)\left(v_{\infty,A,T}\right)^2}{\mu}}\right) \tag{61}$$

and

$$\eta_D = \cos^{-1}\left(\frac{-1}{1 + \frac{\left(r_{\pi,T}{}^{c}\right)\left(v_{\infty,D,T}\right)^2}{\mu}}\right) \tag{62}$$

For the given flight times $t_T$ and $t_R$ and stay time $t_S$, the computed radius of periapsis $r_{\pi,T}{}^{c}$ is a function of the velocity vectors $\vec{v}_{\infty,A,T}$ and $\vec{v}_{\infty,D,T}$ only. Equations (59) to (62) may be solved iteratively for $r_{\pi,T}{}^{c}$ by using a Newton-Raphson technique.

A second iteration is required in order to satisfy the constraint

$$h_{\pi,T} - h_{\pi,T}{}^{c} = 0 \tag{63}$$

This constraint may be satisfied either by permitting $t_T$ to be free and constraining the total time, or by permitting $t_R$ to be free and constraining $t_T$. The computation

is similar to the computation for the parking orbit about an oblate planet, which is discussed in the previous section of this report.

## EXAMPLE PROBLEMS

Three examples were chosen to illustrate the use of the matching technique discussed in this report. In each example, the departure date and launch times were chosen from recent literature or from unpublished studies. The flight times were adjusted during the computation process in order to satisfy the mission constraints. The purpose of the examples is not to present a comparison between the flight times chosen from the literature and the flight times computed by the iteration techniques discussed previously, but to demonstrate that continuous matched-conic solutions to round-trip trajectory problems can be generated from flight times that are only approximately known.

The first example, presented in table I, is an Earth-Mars-Earth free-flyby trajectory. The data for this trajectory were chosen from reference 9. The initial guesses for flight times were found to be 130 days from Earth to Mars and 540 days for the return to Earth for an Earth departure date of Julian date 2 442 670. In table I, it is indicated that these times were changed to 136.61225 and 539.64008 days, respectively, in order to satisfy the constraints. The flyby and altitude constraints presented in equations (37) and (38) were satisfied to $10^{-3}$ fps and $10^{-4}$ nautical miles, respectively. The boundary conditions were $i_D = 35°$, $i_R = 50°$, $h_{\pi, D} = 262$ nautical miles, $h_{\pi, R} = 50$ nautical miles, and $h_{\pi, T} = 200$ nautical miles. The periapsis at departure and at return was chosen for a minimum declination $\left(k_D = 0 \text{ and } k_R = 0\right)$.

The second example, presented in table II, was chosen from reference 10. This stopover trajectory is of the low-energy, conjunction-class of Mars missions. The flight times were chosen to be 302 days from Earth to Mars and 321 days for the return to Earth. The Earth departure date is Julian date 2 444 930, and the stay time at Mars was chosen to be 416 days. The oblateness of Mars was used in order to rearrange the orientation of the parking orbit at its periapsis so that no plane changes were required. The time to return was allowed to be free in order to satisfy the integral orbit constraint presented in equation (56). The return time was changed to 321.8555 days, and the chosen parking-orbit solution had an eccentricity of 0.781518 and an inclination to the Mars equator of 146.580°. The boundary conditions were $i_D = 70°$, $i_R = 75°$, $h_{\pi, D} = 262$ nautical miles, $h_{\pi, R} = 20$ nautical miles, and $h_{\pi, T} = 200$ nautical miles. The periapsis at the departure planet was chosen to have a minimum $\left(k_D = 0\right)$ declination, and the periapsis at the return planet was chosen to have a maximum $\left(k_R = 1\right)$ declination.

The third example, presented in table III, is an example of a parking orbit with coincident periapsis of the arrival and departure legs at the target planet. The departure planet is Mars, the target planet is Venus, and the return planet is Earth. The

initial guesses for the flight times were 260 days from Mars to Venus and 170 days from Venus to Earth. The departure date at Mars was chosen to be Julian date 2 443 493, and the stay time at Venus was chosen to be 10 days. The total flight time was held constant, and the flight times were changed to 270.68412 and 169.31588 days in order to satisfy the constraint, presented in equation (63), for the specified periapsis altitude. In order to obtain a highly elliptical orbit, the period of the parking orbit was chosen to be one-third of the specified stay time. The boundary conditions were $i_D = 40°$, $i_R = 40°$, $h_{\pi, D} = 150$ nautical miles, $h_{\pi, R} = 50$ nautical miles, $h_{\pi, T} = 200$ nautical miles, $k_D = 0$, and $k_R = 0$.

## CONCLUDING REMARKS

A technique for matching conic trajectories at the gravitation sphere-of-influence boundaries is presented. The matching is made, with continuity in position, velocity, and time at the sphere-of-influence boundaries insured. The technique is extended to several types of round-trip planetary missions and has the capability of satisfying in-flight constraints at the target planet. The types of missions considered are the free-flyby mission, the powered-flyby mission, and the stopover mission with a parking orbit about the target planet. An example is presented of each mission type.

The chief advantage of the technique is its capability of being adapted to several mission types. The single-leg matched-conic trajectory can be used to obtain other types of solutions, for example, the optimum powered-flyby trajectory. The requirement for its use in obtaining other solutions is that the constraints be properly identified and stated mathematically. The limitations of this technique are no more severe than those for any other matched conic; that is, the technique represents only an approximation to the precision-integrated trajectory.

Manned Spacecraft Center
National Aeronautics and Space Administration
Houston, Texas, August 19, 1968
981-30-10-00-72

## REFERENCES


1. Knip, G., Jr.; and Zola, C. L.: Three-Dimensional Sphere-of-Influence Analysis of Interplanetary Trajectories to Mars. NASA TN D-1199, 1962.

2. Battin, R.; and Miller, J.: Circumlunar Trajectory Calculations. MIT Instrumentation Laboratory Report R-543, April 1962.

3. Battin, Richard H.: Astronautical Guidance. McGraw-Hill Book Co., Inc., 1964.

4. Luidens, Roger W.; and Kappraff, Jay M.: Mars Nonstop Round-Trip Trajectories. NASA TN D-2605, 1965.

5. Willis, Edward A., Jr.: Optimization of Double-Conic Interplanetary Trajectories. NASA TN D-3184, 1966.

6. Margenau, Henry; and Murphy, George M.: The Mathematics of Physics and Chemistry. D. Van Nostrand Co., Inc., 1956.

7. Danby, John M. A.: Fundamentals of Celestial Mechanics. The MacMillan Company, 1962.

8. Thibodeau, Joseph R.: Use of Planetary Oblateness for Parking-Orbit Alinement. NASA TN D-4657, 1968.

9. Ross, S.: Planetary Flight Handbook. NASA SP-35, vol. 3, 1963.

10. Lee, Vernon A.; and Wilson, Sam W., Jr.: A Survey of Ballistic Mars-Mission Profiles. J. Spacecraft and Rockets, vol. 4, no. 2, Feb. 1967, pp. 129-142.

TABLE I. - EARTH-MARS-EARTH FREE-FLYBY TRAJECTORY FOR AN EARTH DEPARTURE DATE OF SEPTEMBER 14, 1975 (JULIAN DATE 2 442 670.0)[a]

| Location (coordinate system) | Time from departure periapsis, days | Position vector (b, c) | | | | Velocity vector, fps (c) | | | |
|---|---|---|---|---|---|---|---|---|---|
| | | X | Y | Z | Magnitude | $\dot{X}$ | $\dot{Y}$ | $\dot{Z}$ | Magnitude |
| Earth periapsis (planetocentric) | 0.0000000 | 2885.0346 | -1531.3456 | -1750.8615 | 3705.9361 | 23741.259 | 29758.012 | 13093.283 | 40256.933 |
| Exit Earth sphere of influence (planetocentric) | 1.7417041 | -7409.3675 | 417898.25 | 273257.02 | 499362.84 | -580.81599 | 16264.951 | 10712.090 | 19484.220 |
| Exit Earth sphere of influence (heliocentric) | 1.7417041 | 0.99728074 | -0.12075733 | 0.00104548 | 1.0045657 | 10155.239 | 115785.87 | 3357.2698 | 116278.84 |
| Enter Mars sphere of influence (heliocentric) | 135.82706 | -0.39312709 | 1.5504021 | 0.042567679 | 1.6000336 | -78956.047 | 14540.547 | 59.655663 | 80283.798 |
| Enter Mars sphere of influence (planetocentric) | 135.82706 | -303135.60 | -51517.335 | 52282.088 | 311895.24 | 27037.989 | 4771.2949 | -4550.4197 | 27830.278 |
| Mars periapsis (planetocentric) | 136.61225 | 160.34837 | 1736.1971 | 1066.6065 | 2043.9524 | 30935.784 | 1786.1843 | -7558.2427 | 31895.771 |
| Exit Mars sphere of influence (planetocentric) | 137.39745 | 296818.96 | -16876.856 | -94299.085 | 311895.24 | 26441.853 | -1683.4489 | -8515.7992 | 27830.278 |
| Exit Mars sphere of influence (heliocentric) | 137.39745 | -0.41436130 | 1.5542281 | 0.41691174 | 1.6090551 | -74638.109 | 12882.585 | -6356.1945 | 76007.956 |
| Enter Earth sphere of influence (heliocentric) | 675.14776 | 0.47414165 | -0.90459878 | -0.00233758 | 1.0213299 | 83433.957 | 74223.266 | 11706.371 | 112282.49 |
| Enter Earth sphere of influence (planetocentric) | 675.14776 | 27632.274 | -348254.19 | -356817.50 | 499362.84 | -1432.8183 | 21953.590 | 22279.237 | 31310.980 |
| Earth periapsis (planetocentric) | 676.25233 | 2790.5805 | 2099.9400 | 102.48199 | 3493.9361 | -19392.789 | 23980.287 | 36689.108 | 47929.375 |

[a]For this trajectory, $i_D = 35°$, $i_R = 50°$, $h_{\pi,D} = 262$ n. mi., $h_{\pi,R} = 50$ n. mi., $h_{\pi,T} = 200$ n. mi., $k_D = 0$, and $k_R = 0$.

[b]Planetocentric position vectors are measured in nautical miles. Heliocentric position vectors are measured in astronomical units.

[c]Planetocentric vectors are in the planetocentric equatorial (Earth equatorial at Earth, Mars equatorial at Mars) system. Heliocentric vectors are in the heliocentric ecliptic system.

TABLE II. - MARS STOPOVER TRAJECTORY FOR AN EARTH DEPARTURE DATE OF NOVEMBER 21, 1981 (JULIAN DATE 2 444 930.0)[a]

| Location (coordinate system) | Time from departure periapsis, days | Position vector (b, c) | | | | Velocity vector, fps (c) | | | |
|---|---|---|---|---|---|---|---|---|---|
| | | X | Y | Z | Magnitude | $\dot{X}$ | $\dot{Y}$ | $\dot{Z}$ | Magnitude |
| Earth periapsis (planetocentric) | 0.0000000 | 2203.8515 | 1089.0369 | -2773.2652 | 3705.9361 | -29481.566 | 6540.4417 | -20859.963 | 36702.563 |
| Exit Earth sphere of influence (planetocentric) | 3.1134812 | -462994.31 | -78452.616 | 169837.30 | 499362.84 | -9444.9839 | -1700.8943 | 3740.5277 | 10300.112 |
| Exit Earth sphere of influence (heliocentric) | 3.1134812 | .45392720 | .87354679 | .00231538 | .98444870 | -97533.951 | 45080.633 | 4108.2831 | 107526.80 |
| Enter Mars sphere of influence (heliocentric) | 299.86212 | .18029548 | -1.4286007 | -.03421212 | 1.4403391 | 72089.638 | 14845.003 | -2083.5210 | 73631.725 |
| Enter Mars sphere of influence (planetocentric) | 299.86212 | 64926.100 | -270147.78 | 141715.98 | 311895.24 | -2190.0579 | 8626.0528 | -4586.8241 | 10012.197 |
| Mars periapsis (planetocentric) | 302.00000 | -1729.9204 | 320.21172 | -1040.4716 | 2043.9524 | 5549.2527 | 17229.915 | -3923.7452 | 18521.877 |
| In parking orbit | 302.00000 | -1729.9204 | 320.21172 | -1040.4716 | 2043.9524 | 4420.7970 | 13726.165 | -3125.8409 | 14755.403 |
| Out of parking orbit | 718.00000 | -626.75358 | 1646.2809 | 1036.6680 | 2043.9523 | 14016.807 | 3326.9259 | 3191.0204 | 14755.403 |
| Mars periapsis (planetocentric) | 718.00000 | -626.75358 | 1646.2809 | 1036.6680 | 2043.9523 | 16517.016 | 3920.3572 | 3760.2100 | 17387.357 |
| Exit Mars sphere of influence (planetocentric) | 720.73968 | 284451.20 | -115326.59 | -55370.858 | 311895.24 | 6988.1476 | -2937.4740 | -1428.7832 | 7713.9083 |
| Exit Mars sphere of influence (heliocentric) | 720.73968 | -1.4095229 | .88520748 | .05195948 | 1.6652467 | -36745.480 | -53721.482 | -2739.5946 | 65143.943 |
| Enter Earth sphere of influence (heliocentric) | 1037.95365 | .99805264 | .02744371 | -.00191360 | .99843170 | 7751.2668 | 108673.38 | 5767.1951 | 109102.00 |
| Enter Earth sphere of influence (planetocentric) | 1037.9537 | -350685.71 | -232226.83 | -269171.84 | 499362.84 | 12405.649 | 8111.4572 | 9803.2147 | 17770.731 |
| Earth periapsis (planetocentric) | 1039.8555 | 979.42250 | -294.46639 | 3309.5128 | 3463.9362 | 28086.748 | 28671.900 | -5760.9329 | 40547.892 |

[a]For this trajectory, $i_D = 70°$, $i_R = 75°$, $h_{\pi,D} = 262$ n. mi., $h_{\pi,R} = 20$ n. mi., $h_{\pi,T} = 200$ n. mi., $k_D = 0$, and $k_R = 1$.

[b]Planetocentric position vectors are measured in nautical miles. Heliocentric position vectors are measured in astronomical units.

[c]Planetocentric vectors are in the planetocentric equatorial (Earth equatorial at Earth, Mars equatorial at Mars) system. Heliocentric vectors are in the heliocentric ecliptic system.

TABLE III. - MARS-VENUS-EARTH TRAJECTORY WITH PARKING ORBIT (PERIOD = 80 HR) ABOUT VENUS

FOR A MARS DEPARTURE DATE OF DECEMBER 15, 1977 (JULIAN DATE 2 443 493)[a]

| Location (coordinate system) | Time from departure periapsis, days | Position vector (b, c) | | | | Velocity vector, fps (c) | | | |
|---|---|---|---|---|---|---|---|---|---|
| | | X | Y | Z | Magnitude | $\dot{X}$ | $\dot{Y}$ | $\dot{Z}$ | Magnitude |
| Mars periapsis (planetocentric) | 0.0000000 | -1610.4360 | -487.51092 | -1069.8950 | 1993.9524 | 1013.3574 | -19876.006 | 7531.4149 | 21279.209 |
| Exit Mars sphere of influence (planetocentric) | 1.5161525 | 107898.95 | -241735.97 | 164924.76 | 311895.24 | 5038.6730 | -10987.367 | 7599.3071 | 14277.953 |
| Exit Mars sphere of influence (heliocentric) | 1.5161525 | -0.41311593 | 1.5511198 | 0.04336610 | 1.6057765 | -60281.586 | -9563.6723 | 3677.5070 | 61146.197 |
| Enter Venus sphere of influence (heliocentric) | 259.57448 | 0.31693437 | -0.64791667 | -0.02717924 | 0.72179090 | 121655.43 | 58789.120 | -.69779800 | 135295.58 |
| Enter Venus sphere of influence (planetocentric) | 259.57448 | -312425.87 | -113050.52 | -24215.915 | 333131.74 | 19111.048 | 6980.4972 | 1082.4660 | 20374.769 |
| Venus periapsis (planetocentric) | 260.68412 | 1867.3431 | 1144.4505 | -2722.0318 | 3493.7364 | 29696.826 | 7289.7737 | 2343.7253 | 38527.226 |
| In parking orbit | 260.68412 | 1867.3431 | 1144.4505 | -2722.0318 | 3493.7364 | 24867.625 | 6104.3343 | 1962.5964 | 32262.053 |
| Out of parking orbit | 270.68412 | 1867.3088 | 1144.4522 | -2722.0546 | 3493.7364 | 24867.625 | 6104.3343 | 1962.5964 | 32262.053 |
| Venus periapsis (planetocentric) | 270.68412 | 1867.3088 | 1144.4522 | -2722.0546 | 3493.7364 | 29029.799 | 7126.2610 | 22910.365 | 37661.619 |
| Exit Venus sphere of influence (planetocentric) | 271.88744 | 99235.993 | -14784.617 | 317670.21 | 333131.75 | 5212.7837 | -977.51682 | 17917.953 | 18686.404 |
| Exit Venus sphere of influence (heliocentric) | 271.88744 | .52094398 | -.49653745 | -0.03319247 | 72044000 | 84352.754 | 90040.293 | 13425.145 | 124108.32 |
| Enter Earth sphere of influence (heliocentric) | 437.82797 | -.91598292 | .38231432 | .00423224 | 0.99257587 | -30201.160 | -84328.989 | -10552.387 | 90193.354 |
| Enter Earth sphere of influence (planetocentric) | 437.82797 | -300574.20 | -324349.88 | 231981.80 | 499362.84 | 9383.5571 | 9774.8658 | -7263.3681 | 15373.863 |
| Earth periapsis (planetocentric) | 440.00000 | 2672.9480 | -141.85234 | -2245.6217 | 3493.9361 | 2396.8676 | 39336.023 | 368.18051 | 39410.698 |

[a]For this trajectory, $i_D = 40°$, $i_R = 40°$, $h_{\pi,D} = 150$ n. mi., $h_{\pi,R} = 50$ n. mi., $h_{\pi,T} = 200$ n. mi., $k_D = 0$, and $k_R = 0$.

[b]Planetocentric position vectors are measured in nautical miles. Heliocentric position vectors are measured in astronomical units.

[c]Planetocentric vectors are in the planetocentric equatorial (Earth equatorial at Earth and Venus, Mars equatorial at Mars) system. Heliocentric vectors are in the heliocentric ecliptic system.

NATIONAL AERONAUTICS AND SPACE ADMINISTRATION
WASHINGTON, D. C. 20546

OFFICIAL BUSINESS

FIRST CLASS MAIL

POSTAGE AND FEES PAID
NATIONAL AERONAUTICS AND
SPACE ADMINISTRATION



*"The aeronautical and space activities of the United States shall be conducted so as to contribute . . . to the expansion of human knowledge of phenomena in the atmosphere and space. The Administration shall provide for the widest practicable and appropriate dissemination of information concerning its activities and the results thereof."*

— NATIONAL AERONAUTICS AND SPACE ACT OF 1958

# NASA SCIENTIFIC AND TECHNICAL PUBLICATIONS

TECHNICAL REPORTS: Scientific and technical information considered important, complete, and a lasting contribution to existing knowledge.

TECHNICAL NOTES: Information less broad in scope but nevertheless of importance as a contribution to existing knowledge.

TECHNICAL MEMORANDUMS: Information receiving limited distribution because of preliminary data, security classification, or other reasons.

CONTRACTOR REPORTS: Scientific and technical information generated under a NASA contract or grant and considered an important contribution to existing knowledge.

TECHNICAL TRANSLATIONS: Information published in a foreign language considered to merit NASA distribution in English.

SPECIAL PUBLICATIONS: Information derived from or of value to NASA activities. Publications include conference proceedings, monographs, data compilations, handbooks, sourcebooks, and special bibliographies.

TECHNOLOGY UTILIZATION PUBLICATIONS: Information on technology used by NASA that may be of particular interest in commercial and other non-aerospace applications. Publications include Tech Briefs, Technology Utilization Reports and Notes, and Technology Surveys.

*Details on the availability of these publications may be obtained from:*

**SCIENTIFIC AND TECHNICAL INFORMATION DIVISION**

**NATIONAL AERONAUTICS AND SPACE ADMINISTRATION**

**Washington, D.C. 20546**